Journal of the Korea Concrete Institute
Vol.15 No.6, pp.915-923, December, 2003

Tension Stiffening Effect of High-Strength Concrete in Axially Loaded Members

Woo Kim[1)*], Ki-Yeol Lee[1)], and Hwan-Seok Yum[2)]

[1)] *Department of Civil Engineering, Chonnam National University, Korea*
[2)] *Division of Architecture, Gwangju University, Korea*

(Received May 25, 2003; Accepted October 30, 2003)

Abstract

This paper presents the test results of total 35 direct tensile specimens to investigate the effect of high-strength concrete on the tension stiffening effect in axially loaded reinforced concrete tensile members. Three kinds of concrete strength 25, 60, and 80 MPa were included as a major experimental parameter together with six concrete cover thickness ratios. The results showed that as higher strength concrete was employed, not only more extensive split cracking along the reinforcement was formed, but also the transverse crack space became smaller. Thereby, the effective tensile stiffness of the high-strength concrete specimens at the stabilized cracking stage was much smaller than those of normal-strength concrete specimens. This observation is contrary to the current design provisions, and the significance in reduction of tension stiffening effect by employment of high-strength concrete is much higher than that would be expected. Based on the present results, a modification factor is proposed for accounting the effect of the cover thickness and the concrete strength.

Keywords : bond, cover thickness, crack space, high-strength concrete, tension stiffening effect

1. Introduction

In the conventional methods for designing reinforced concrete members the concrete tensile resistance in a section is generally neglected, and the force equilibrium condition is only considered. By the recent trend of the employing more accurate analysis such as strength design methods as well as higher strength materials, smaller member sizes and higher tension stress in reinforcement are resulted in. Thereby, it is getting to increase the necessity of taking into account for the deformation compatibility conditions in designing reinforced concrete structures.

When a reinforced concrete member is cracked, the stiffness is drastically decreased and the internal stresses are redistributed in such a way that in the cracked cross-section all sectional force is resisted by the steel only, while in the part between adjacent cracks, a part of tensile forces is transmitted from the steel to the surrounding concrete through the bond. Thus the concrete between cracks contributes to increase the stiffness of the tensile reinforcement, and this effect is normally called the tension stiffening effect[1)].

As shown in Fig. 1, the cracking behavior and the stiffness of a tension member depends mostly on bond characteristics at the interface between the concrete and the rebar. When the first crack occurs, the distribution of strains in the steel and the concrete as in Fig. 1b, can be divided into two parts of the stress disturbed region (D-region), where the strains vary, and the stress continuity region(B-region), where the strains are uniform along the section. The strains in D-region depend on the distribution of bond stress u within the transmission length l_t. As indicated in Fig. 1*d*, the cracking continues until the whole member consists of overlapping D-regions.

The smallest possible crack distance is found just at the end of a D-region. And the maximum crack distance will be $2l_t$. Thus the crack distance varies between l_t and $2l_t$. A summary of research carried on tension stiffening and cracking of structural concrete in direct tension is given by ACI Committee 224[2)] and CEB Manual.[3)]

* *Corresponding author*
Tel.: +82-62-530-1655; Fax.: +82-62-530-1659
E-mail address: wkim@chonnam.ac.kr

According to the design code for tension stiffening of tension member in MC-90(CEB-FIB MODEL CODE 199 0), the overall tension stiffening behavior is divided into 4 loading stages and expressed in term of the mean steel strain ε_{sm} as shown in Fig. 2.

The average strain in the reinforcement in the stabilized stage is given by

$$\varepsilon_{sm} = \varepsilon_{so} - \beta_t \frac{f_{ct}}{E_s \rho} \quad (1)$$

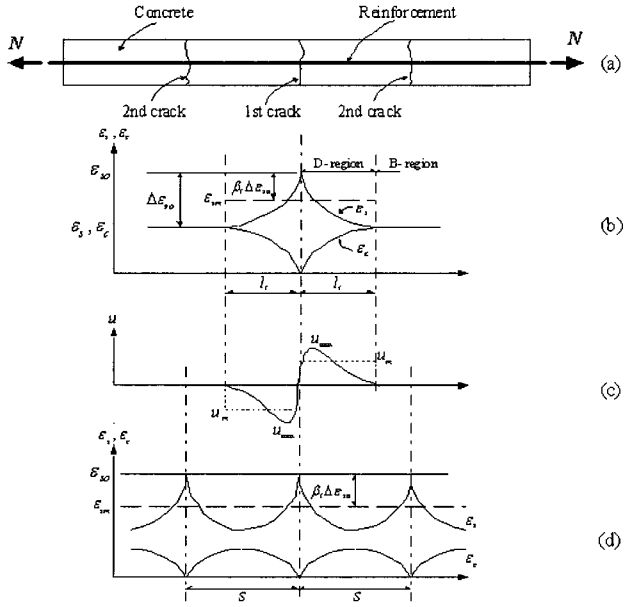

Fig. 1 Distribution of Stress and Strain in Tension Members (CEB-FIP MODEL CODE 1990)
(a) Tension Member, (b) Single Crack Stage,
(b) Bond Stress at Single Crack Stage,
(d) Stabilized Crack Stage

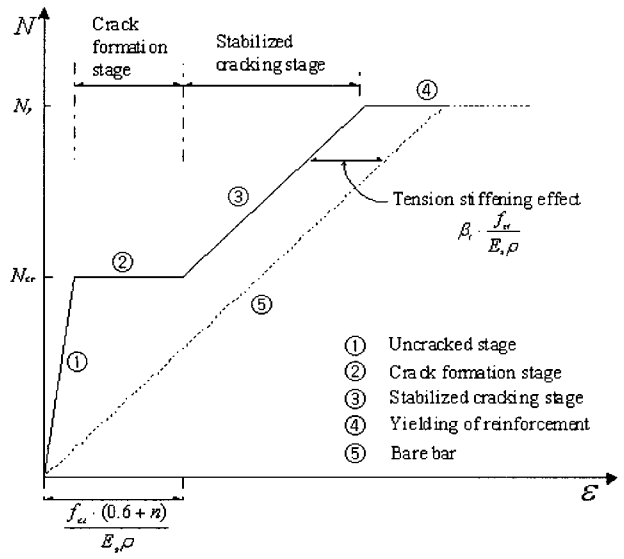

Fig. 2 Simplified load-deformation relation for a centrically reinforced member subjected to tension defined by MC-90

Where ε_{so} is the strain in reinforcement at the crack section, β_t is an experimental constant accounting for the effects of tension stiffening with 0.40 for short term loading, and 0.25 for long-term or repeated loading, f_{ct} is the tensile strength of concrete, E_s is the modulus of elasticity of steel, and ρ is the ratio of reinforcement.

Eq. (1) is a simple expression based on the work carried out by Leonhardt[4] and Stroband[5]. But their work did not include two major parameters of cover thickness and concrete strength influencing the tension stiffening effect. The split cracking resulted from a thin cover thickness of concrete is considerably influencing the tensile stiffness of axially loaded members in which transverse cracks and splitting cracks occur intricately. The experimental investigation carried out by Abrishami and Mitchell[6] showed a significant reduction in the tension stiffness by the split cracking along the reinforcement, and they suggested that the influence should be taken into account unless the cover to bar diameter ratio c/d_b is more than 2.5.

Eq. (1) also cannot express the effect of the concrete strength that may alter the bond characteristics. The work done by Azizinamini[7] and Hungspreug[8] indicated that, as shown in Fig. 3, as higher strength concrete was employed, not only peak bond stress became higher, but also more extensive concentration near the loaded end was resulted in. These characteristics in bond behavior of high-strength concrete can be quantitatively drawn from the elastic theory. Since the elastic modulus of concrete is a function of compressive strength, while that of steel remains constant, the composite structural system consisted of reinforcement and concrete is altered with concrete strength, so that different stress state in the interface is resulted in. Moreover, high-strength concrete is generally more brittle than normal-strength concrete, and in turns, smaller stress redistribution will be expected at the ultimate loading stages.

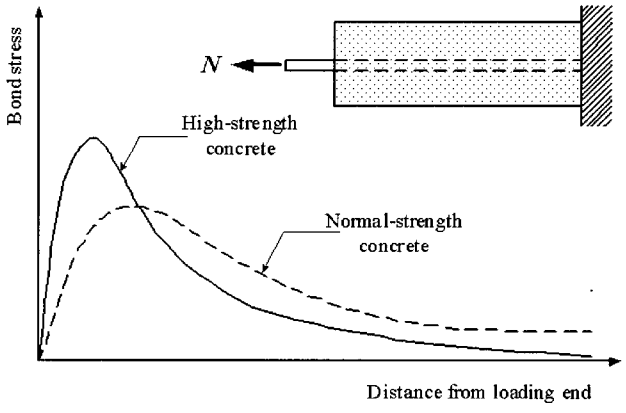

Fig.3 Bond stress distribution of pullout test

These two material aspects in high-strength concrete may lead to making D-region shorter, thus, the crack space as well as the effective tensile stiffness of axially loaded members may change.

Hence, in the present study an experimental work was planned to evaluate the tension stiffness of axially loaded members of high-strength concrete. Direct tension tests were performed with three kinds of concrete strength and six kinds of the cover thickness to bar diameter ratio (c/d_b) as major variables. Using the result obtained from the experiments, the cracking behavior and the effect of tension stiffening were examined.

2. Experimental work

The test specimens in this study were, as shown in Fig. 4, axially loaded direct tension members with the length of 150 cm, and one D19 bar of SD 40 at the center of the rectangular section. The sectional area of the specimen kept constant of 232.5 cm^2 in all specimens, but had rectangular shapes with different aspect ratios in order to vary the cover thickness of c/d_b between 1.0 and 3.5 with 0.5 increments.

The concrete mix design is shown in Table 1, with three types of normal-strength concrete (NSC, 25 MPa), medium-strength concrete (MSC, 60 MPa), and high-strength concrete (HSC, 80 MPa). All properties of 35 specimens were listed in Table 2. To minimize the shrinkage during the curing procedure, wet curing was done for 3 days after concrete casting until demoulding, and afterwards submerged curing was provided for 4 to 6 weeks until the test.

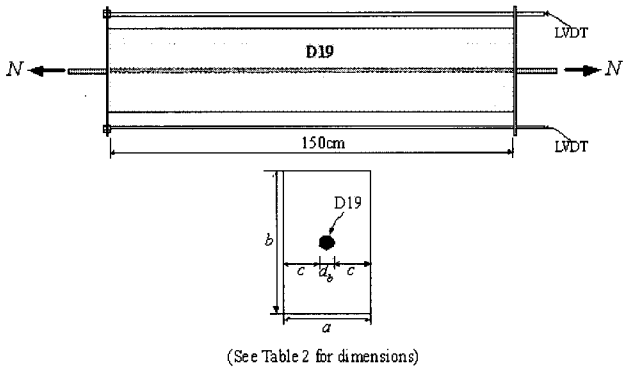

(See Table 2 for dimensions)

Fig. 4 Specimen geometry

For the loading a displacement control method was employed, and the longitudinal elongation between the both ends of each specimen was measured as in Fig. 4, with four electrical displacement transducers(LVDT) mounted at each corner. Then the mean value was used to plot the load-deformation curve for each specimen. The cracks observed during the loading were marked and used in investigating the overall cracking behavior.

3. Results and discussion

3.1 Effect of cover thickness

The load-deformation curves obtained from the experiments are shown in Fig. 5. The comparison of the curves resulted from having different cover thickness shows that in spite of the same sectional area and steel ratio the axial stiffness becomes significantly higher with increasing the cover thickness. The load at which the first transverse crack was observed is defined as the transverse cracking load N_{tr}, and the load for the first cracking along the rebar is also defined as the split cracking load N_{sp} for each specimen, and listed in Table 2. These are also marked on the curves in Fig. 5, and show that the axial deformation after cracking is highly depending on the thickness of concrete cover.

From the curves of the normal strength concrete (f_{ck} = 25 MPa) specimens in Fig. 5a, it is clear that the N_{tr} of every 6 specimens were nearly identical, while the split cracking load N_{sp} varied significantly with the cover thickness. In the specimen having thin cover thickness (c/d_b = 1.0 and 1.5), the splitting crack appeared earlier than the transverse crack did, and extended along the bar. Thus, the larger deformation was resulted in, and the effect of tension stiffening was small. To the contrary, in the specimens with thick cover thickness (c/d_b = 3.0 and 3.5) the splitting crack appeared at much higher loading stage, and those cracks did not affect the axial stiffness of the members. Fig. 5b shows the load-deformation curves of the specimens with high strength concrete (f_{ck} = 80 MPa). Comparing Fig. 5b with Fig. 5a, it can be observed that the axial strain in high strength concrete is much larger than those in the normal strength concrete at the crack stabilizing stage although the concrete compressive strength is three times higher.

Table 1 Mixture design of concrete

Design strength (MPa)	W/C	S/A (%)	Slump (cm)	Unit weight (kgf/m^3)				Admixture (kgf/m^3)		Test strength (MPa)
				C	W	S	G	S.F	M-150	
25	0.60	45	15	385	229	810	991	0	0	24.8
55	0.25	37	15	550	138	662	1105	0	11	60.7
85	0.20	38	15	650	153	578	950	98	13	80.4

Note) C: cement, W: water, S: sand, G: gravel, S.F: silica fume, M-150: supper plasticizer

Table 2 Specimen properties and test results

Specimens	Cover thickness ratio (c/d_b)	Cross sectional dimensions $a \times b$ (mm)	Measured concrete strength		Initial cracking load		Number of transverse crack (each)	Average crack spacing (cm)	Length of splitting crack cm (%)
			Compressive strength f_{ck} (MPa)	Tensile strength f_{sp} (MPa)	Transverse crack N_{tr} (kN)	Splitting crack N_{sp} (kN)			
N 10-A	1.0	60 ×385	24.8	1.96	55	42	7	18.8	65(43)
N 10-B					54	36	10	13.6	69(46)
N 15-A	1.0	80 ×290			55	39	8	16.7	72(48)
N 15-B					46	46	12	11.5	81(54)
N 20-A	2.0	100 ×230			51	53	10	13.6	76(51)
N 20-B					48	62	9	15.0	59(39)
N 25-A	2.5	115 ×200			52	68	7	18.8	51(34)
N 25-B					47	84	9	15.0	29(19)
N 30-A	3.0	135 ×170			51	84	6	21.4	35(23)
N 30-B					52	86	5	25.0	26(17)
N 35-A	3.5	150 ×155			45	93	4	30.0	5(3)
N 35-B					50	93	6	21.4	18(12)
M 10-A	1.0	60 ×385	60.7	3.34	60	41	11	12.5	110(73)
M 15-A	1.5	80 ×290			76	46	12	11.5	101(67)
M 15-B					75	37	15	9.4	116(77)
M 20-A	2.0	100 ×230			62	42	14	10.0	77(51)
M 20-B					71	46	14	10.0	88(59)
M 25-A	2.5	115 ×200			73	69	11	12.5	84(56)
M 25-B					81	64	14	10.0	68(45)
M 30-A	3.0	135 ×170			71	77	13	10.7	76(51)
M 30-B					79	80	9	15.0	68(45)
M 35-A	3.5	150 ×155			77	85	10	13.6	66(44)
M 35-B					77	84	8	16.7	54(36)
H 10-A	1.0	60 ×385	80.4	3.53	68	50	11	12.5	102(68)
H 10-B					73	44	14	10.0	117(78)
H 15-A	1.5	80 ×290			71	54	16	8.8	100(67)
H 15-B					73	48	16	8.8	107(72)
H 20-A	2.0	100 ×230			83	64	15	9.4	106(71)
H 20-B					81	64	16	8.8	110(73)
H 25-A	2.5	115 ×200			86	86	12	11.5	85(53)
H 25-B					81	72	14	10.0	90(60)
H 30-A	3.0	135 ×170			94	94	12	11.5	47(31)
H 30-B					94	94	9	15.0	50(33)
H 35-A	3.5	150 ×155			94	94	12	11.5	38(25)
H 35-B					97	97	13	10.7	37(25)

Note : In all specimens, a D19 was placed at the center of the section (f_y = 430 MPa, ρ = 0.0124)

This result is obviously contrary to that predicted by the current code provisions of Eq. (1). Another important thing that can be observed in Fig. 5b is that in the HSC specimens the split crack appeared earlier loading stage than the load of the transverse cracking.

The transverse cracking load and the split cracking load observed in every specimen are plotted in Fig. 6. It can be said that the transverse cracking loads were the almost same regardless of the cover thickness and increased as the concrete strength became higher.

This was quite natural because of the same sectional area and the increase in concrete tensile strength. However, the split cracking loads were not affected by the concrete strength, but increased in proportion to the cover thickness.

It can be observed in Fig. 6a that the intersecting point at which the two lines representing the cracking loads meet is c/d_b = 2.0. This implies that in the NSC specimens with thin cover thickness of c/d_b smaller than 2.0 splitting crack occurred earlier, and resulted in small tension stiffness. While in the specimens with c/d_b > 2.5 the transverse crack formed earlier, and the effect of the crack on the stiffness was insignificant. This result coincides well with the results of Abrishami and Mitchell[6]. However, as the concrete strength increases, the value of c/d_b at the intersecting point

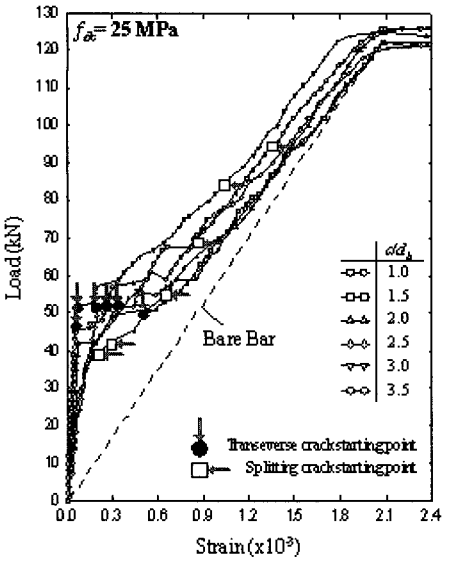

(a) NSC

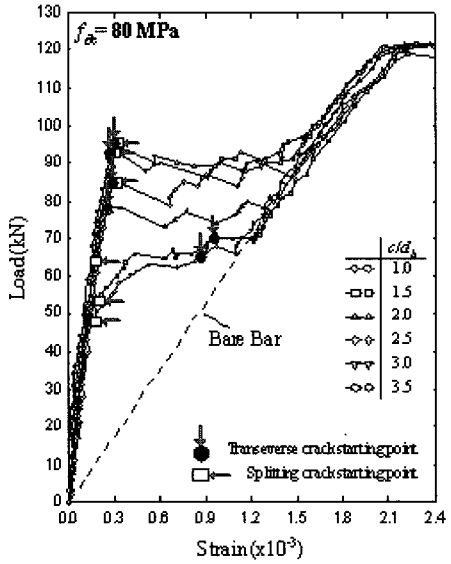

(b) HSC

Fig. 5 Load - deformation curves

becomes higher with 2.5 for MSC and 3.0 for HSC as shown in Fig 6b and 6c. This result indicates that high strength concrete needs thicker cover to prevent split cracking, and hence the criterion of c/d_b = 2.5 which is usually applied to the normal strength concrete is not applied to the high strength concrete.

3.2 Effect of concrete strength

Fig. 7 shows the comparison of the measured load-deformation curves with the predicted curves by Eq. (1) for the specimens having thick cover.

This comparison clearly shows that the effect of tension stiffening at the crack stabilizing stage decreased with increasing concrete strength. This result obviously contradicts to the general knowledge that the effect will be greater in high strength concrete than normal strength concrete because of increase in tensile strength, as predicted by Eq. (1).

The relative cracking loads of MSC and HSC with respect to those in NSC are plotted in Fig. 8.

As the compressive strength of the concrete increased by about 3 times from 25 MPa to 80 MPa, the transverse cracking load increased by approximately 1.9 times, but the split cracking load did not change, and stayed constant. It is noted that the increase ratio in the tensile strength was 1.78 based on the commonly used square root rule between the tensile strength and the compressive strength. From the experimental results, the transverse cracking load in the specimens matches well with the increase ratio in the tensile strength of the concrete, so that the transverse cracking is directly affected by the concrete tensile strength.

However, the split cracking strength did not increase in spite of 1.8 times increase in the concrete tensile strength. From this result, it can be said that the split cracking is not affected by the concrete tensile strength but affected by the thickness of the cover.

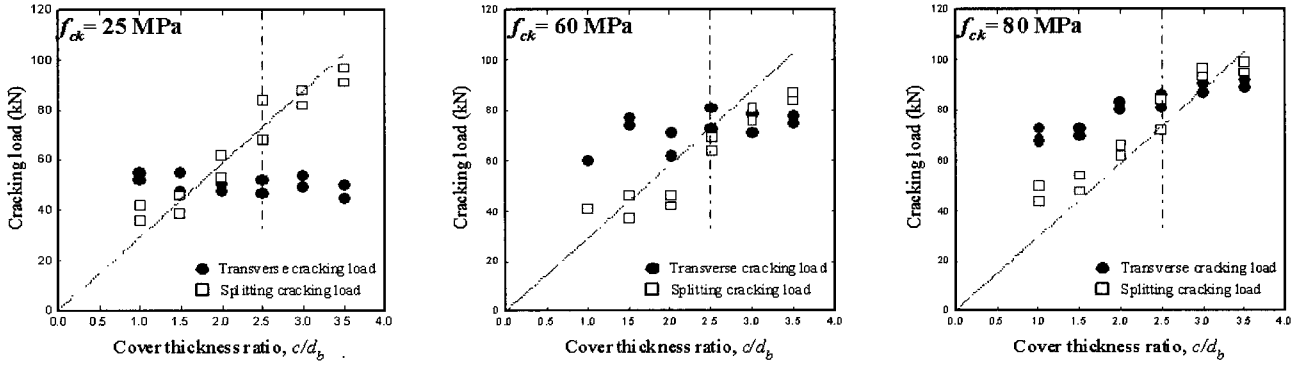

(a) NSC (b) MSC (c) HSC

Fig. 6 Measured variation of transverse cracking load and split cracking load

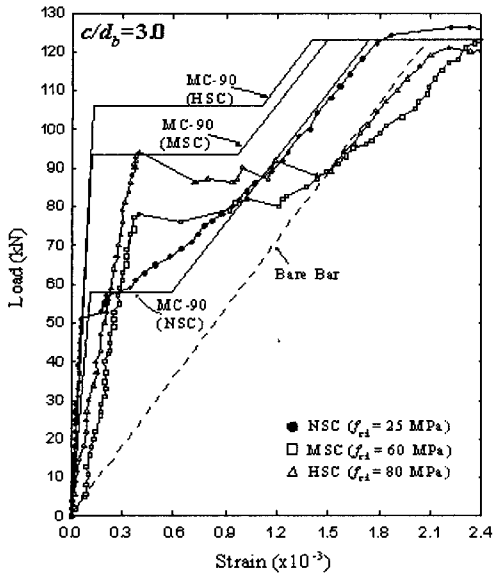

(a) c/d_b = 3.0

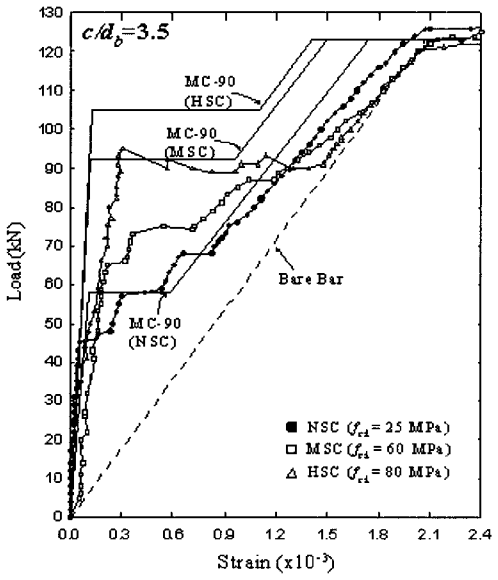

(b) c/d_b = 3.5

Fig. 7 Load - deformation curves

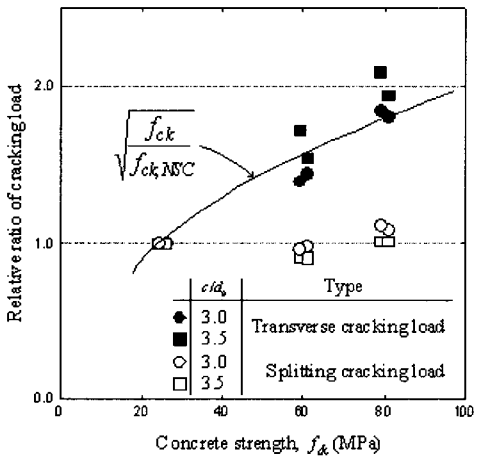

Fig. 8 Relative ratio of cracking loads

From the number of transverse cracks formed up to the yield stage in a specimen, the average distance between adjacent cracks(crack space) is calculated, listed in Table 2, and plotted in Fig. 9. Fig. 10, also shows the final crack configuration for each specimen. These results show that the crack space becomes larger with the increase in cover thickness. This result agrees well with other results published including Broms[9-10]. It can be noted that the wider crack space in the specimen with the thinnest cover (c/d_b = 1.0) may be attributed to the excessive split cracking at the early loading stage.

One of the important facts observed in Fig. 9 and 10 is that the crack space significantly decreases with the increase in concrete strength. As the concrete compressive strength varied from 25 MPa to 80 MPa, the crack space decreased by 30 – 50 percent for all of the cover thickness.

This result contradicts to the result of Abrishami and Mitchell[6] that the crack space increases at higher strength concrete.

3.3. Effect of tension stiffening

According to Eq. (1) from MC-90, since tensile strength of concrete f_{ct} is proportional to the compressive strength while the elastic modulus of steel E_s and steel ratio ρ stay constant, the tension stiffening effect should have been large in the HSC specimens. However, the results measured from the experiments showed smaller stiffness, as shown in Fig. 7. As mentioned previously, this is clearly attributed to the early split cracking and excessive progress along the rebar with increase in load. On the concrete split cracking along the rebar, the bond between the bar and the concrete is diminished, so that the concrete is no longer able to share the tensile force, in turns resulting in large deformation with small stiffening effect.

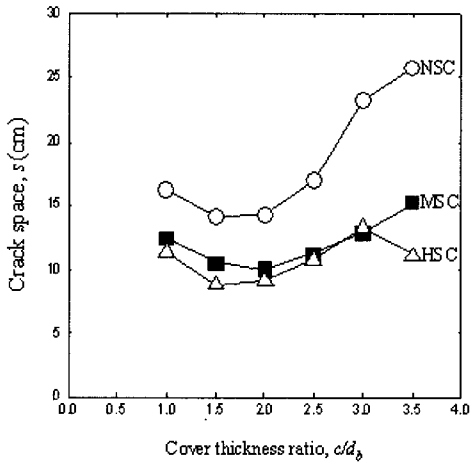

Fig. 9 Average crack space

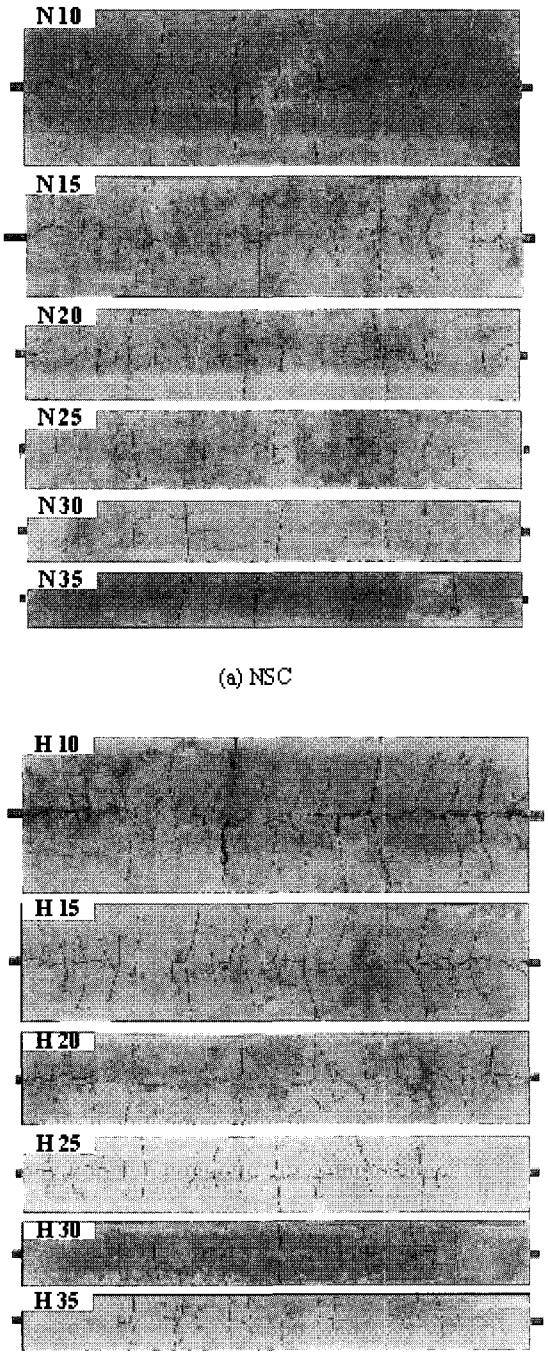

Fig. 10 Final crack configuration

Examining the tension stiffening effect with variation of cover thickness (refer to Fig. 5), it is known that the effect is proportional to the cover thickness, and Eq. (1) is still valid in normal strength concrete. However, in high strength concrete the rate of increase in stiffening effect is much lower than that in normal strength concrete and significantly different values are predicted by Eq. (1). Even in thin covered HSC specimens, there was almost no tension stiffening effect.

From the above results and discussions, it can be concluded that neither the effect of split crack in thin cover thickness nor the material characteristics of high strength concrete is not accounted in Eq. (1). Therefore, any reduction coefficient for accounting those influences should be required to modify Eq. (1).

4. Fomulations

The experimental coefficient β_t in Eq. (1) is fixed with the value of 0.4 for the short-term loading. As discussed previously, the present experimental result shows that the tension stiffness of the axially loaded members is highly dependent on the cover thickness and the concrete strength. And it is observed that the coefficient of 0.4 in Eq. (1) fits appropriately only for the normal strength and for c/d_b value of above 2.5. This observation indicates that tension stiffness of members after cracking cannot be sufficiently predicted by the β_t in Eq. (1), so that additional experimental coefficients should be required to account for the two parameters above. Accordingly, two modification factors are newly added to the β_t in Eq. (1) as the following form, in which the factors $\beta_{t,f_{ck}}$ and $\beta_{t,c/d_b}$ are intended to take into account for the effect of f_{ck} and c/d_b respectively, and each factor has the value of less than unity.

$$\beta_t = 0.4 \cdot \beta_{t,c/d_b} \cdot \beta_{t,f_{ck}} \leq 0.4 \tag{2}$$

The results of the present tests are utilized to evaluate the values of the modification factors in Eq. (2). To derive the value of the factors, Eq. (1) is rearranged for β_t.

$$\beta_t = \frac{E_s \rho}{f_{ct}} (\varepsilon_{so} - \varepsilon_{sm}) \tag{3}$$

Where, E_s = 196,000 MPa, and ρ = 0.0124. For defining f_{ct} the following equation in MC-90 is employed.

$$f_{ct} = f_{cto} \cdot \ln(1 + \frac{f_{ck}}{f_{cko}}) \tag{4}$$

In which f_{cto} = 2.12 MPa, f_{cko} = 10 MPa, and f_{ck} is the compressive strength. Then, by putting the mean ε_{sm} measured at the stabilized stage in each specimen into Eq. (3), β_t can be obtained.

It should be noted here that in every specimen a significant shrinkage strain had been induced during the curing, and resulted in early cracking in the concrete and pre-compressive strain in the reinforcement. For this reason, the deformations of some specimens in Fig. 5 became larger than that of the bare bar. To account for this, the gross shrinkage strain is assumed to be 200×10^{-6} for every specimen, and every measured strain ε_{sm} is adjusted by this amount. As the result of the adjustment, the β_t for the specimen with f_{ck} = 25 MPa and c/d_b of 2.5 becomes 0.4 that is

that is equal to the value given by Eq. (1).

Using the process above, the relationship between the concrete strength and the relative value of $\beta_{t,f_{ck}}$ is determined by a regression analysis of the experimental results as shown in Fig. 11.

It can be seen that the effect of the concrete strength on tension stiffening behavior is directly expressed in a simple form as follows :

$$\beta_{t,f_{ck}} = (\frac{25}{f_{ck}}) \le 1.0 \quad (5)$$

By the same manner, the effect of the cover thickness can be expressed by the following relation as illustrated in Fig. 12. The relation is also compared with the equation suggested by Abrishami and Mitchell[6] that may overestimate the effect of the cover thickness.

$$\beta_{t,c/d_b} = \sqrt{\frac{c/d_b}{2.5}} \le 1.0 \quad (6)$$

This expression is valid for the practical range of c/d_b between 1.0 and 2.5, in which split cracking is probable and affect the stiffness. In summary, a new experimental coefficient β_t to simultaneously account for the effect of the concrete strength as well as the cover thickness can be expressed as follows:

$$\beta_t = 0.4 \cdot \sqrt{\frac{c/d_b}{2.5}} \cdot (\frac{25}{f_{ck}}) \le 0.4 \quad (7)$$

Eq. (1) incorporated with the new experimental coefficient β_t defined by Eq. (7) is examined by applying to the experimental load-deformation curves as illustrated in Fig 13, and it can be seen that the new coefficient provides good predictions at the crack stabilizing stage.

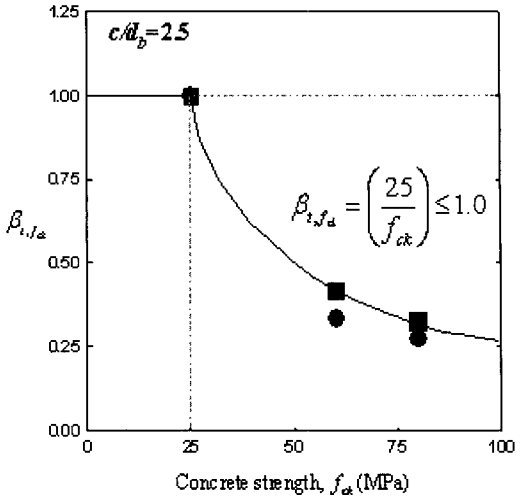

Fig. 11 $\beta_{t,f_{ck}}$ - f_{ck} relation

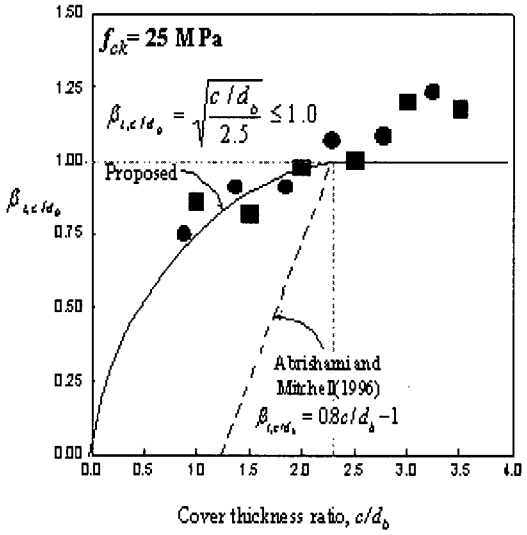

Fig. 12 $\beta_{t,c/d_b}$ - c/d_b Relation

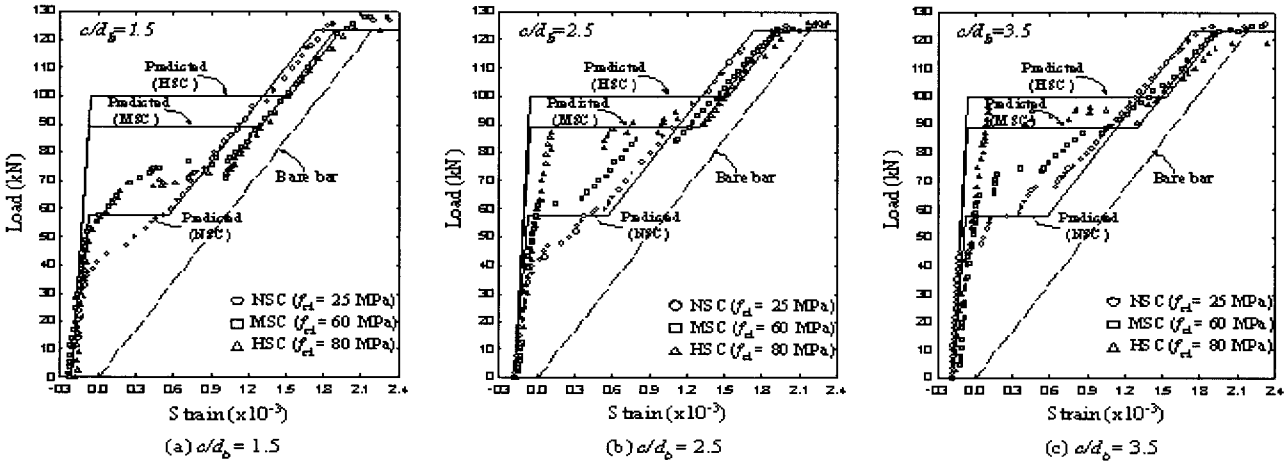

Fig. 13 Comparison between test results and predicted reponse

5. Conclusions

In the present study, total of 35 direct tension tests were performed to investigate the basic behavior of the high strength concrete structure. The strength of concrete and the cover thickness were selected as the main variables to examine the tension stiffening effect, and the followings are drawn.

1) It is observed that the tension stiffening effect is highly dependent on the cover thickness and the concrete strength. As the concrete strength becomes higher, the tension stiffening effect becomes smaller for the practical range of c/d_b less than 2.5. This is clearly attributed to more probable split cracking along the rebar in high-strength concrete.
2) The crack space between the adjacent transverse cracks becomes narrower as higher-strength concrete is used, and the reduction in the crack space was by 30- 50 percent as the concrete compressive strength varied from 25 MPa to 80 MPa.
3) A new experimental factor that can be incorporated with the provisions in MC-90 is proposed. And it can be seen that the new factor provides good predictions for the stiffness at the post-cracking stage in axially tensioned reinforced concrete members.

Acknowledgements

This study was financially supported by Chonnam National University in his sabbatical year of 2003.

References

1. CEB-FIP, "*CEB-FIP Model Code 1990*," Comite Euro-International Du Beton, Paris, 1991.
2. ACI Committee 224, "Cracking of Concrete Members in Direct Tension," *ACI Journal*, Vol.83, No.1, 1986, pp.224.
3. fib(CEB-FIP), "*Structural Concrete-Manual Volume 1*, International Federation for Structural Concrete, " Switzerland, 1999.
4. Leonhardt, F., "*Crack Control in Concrete Structures*," IABSE Surveys No. S-4/77, Zurich, 1977.
5. Stroband, J., "*Experimental Research into theBond Behavior of Reinforcing Bars in Light- weight and Normal Weight Concrete*," Delft University of Technology, Report 25.5-91-3/VF C, 1991.
6. Abrishami, H. H. and Mitchell, D., "Influence of Splitting Cracks on Tension Stiffening," *ACI Structural Journal*, Vol. 93, No.6, 1996, pp.703-710.
7. Azizinamini, A., Stark, M., Roller, J. J., and Ghosh, S. K., "Bond Performance of Reinforcing Bars Embeded in High-Strength Concrete," *ACI Structural Journal*, Vol.90, No.5, 1993, pp.554-561.
8. Hungspreug, S., "*Local Bond Between a Reniforced Bar and Concrete under High Intensity Cyclic Load*," Structural Engineering Report No.81-6, Cornell Unive-rsity, Ithaca, N.Y., 1981.
9. Broms B. B., "Stress Distribution in Reinforced Concrete Member with Tension Cracks," *ACI Structural Journal*, Vol. 62, No.9, 1965, pp.1095-1108.
10. Broms B. B., "Crack Width and Crack Spacing in Reinforced Concrete Members," *ACI Structural Journal*, Vol. 62, No.9, 1965, pp.1237-1256.